ЖЭТФ, 2022, том 162, вып. 4 (10), стр. 466–470

SPIN AND VALLEY EFFECTS ON THE QUANTUM PHASE TRANSITION IN TWO DIMENSIONS

A. A. Shashkin [a*], ***S. V. Kravchenko*** [b**]

[a] *Institute of Solid State Physics, Russian Academy of Sciences*
142432, Chernogolovka, Moscow District, Russia

[b] *Physics Department, Northeastern University*
02115, Boston, Massachusetts, USA

Received June 21, 2022,
revised version June 21, 2022
Accepted June 22, 2022

Contribution for the JETP special issue in honor of E. I. Rashba's 95th birthday

DOI: 10.31857/S0044451022100042
EDN: EMYXXZ

Abstract. Using several independent methods, we find that the metal–insulator transition occurs in the strongly-interacting two-valley two-dimensional electron system in ultra-high mobility SiGe/Si/SiGe quantum wells in zero magnetic field. The transition survives in this system in parallel magnetic fields strong enough to completely polarize the electrons' spins, thus making the electron system "spinless". In both cases, the resistivity on the metallic side near the transition increases with decreasing temperature, reaches a maximum at a temperature T_{max}, and then decreases. The decrease reaches more than an order of magnitude in zero magnetic field. The value of T_{max} in zero magnetic field is found to be close to the renormalized Fermi temperature. However, rather than increasing along with the Fermi temperature, the value T_{max} decreases appreciably for spinless electrons in spin-polarizing magnetic fields. The observed behavior of T_{max} cannot be described by existing theories. The results indicate the spin-related origin of the effect. At the same time, the low-temperature resistivity drop in both spin-unpolarized and spinless electron systems is described quantitatively by the dynamical mean-field theory.

1. Introduction. Spin and valley degrees of freedom in two-dimensional (2D) electron systems have recently attracted much attention due to rapidly developing fields of spintronics and valleytronics (see, e. g., Refs. [1–4]). The existence of the zero-magnetic-field metallic state and the metal–insulator transition (MIT) in strongly interacting 2D electron systems is intimately related to the existence of these degrees of freedom [5–8]. The MIT in two dimensions was theoretically envisioned based on the renormalization group analysis (see Ref. [5] for a review). It was first experimentally observed in a strongly-interacting 2D electron system in silicon metal–oxide–semiconductor field-effect transistors (MOSFETs) [9–12] and subsequently reported in a wide variety of 2D electron and hole systems: p-type SiGe heterostructures, p- and n-type GaAs/AlGaAs heterostructures, AlAs heterostructures, ZnO-related heterostructures etc. (for recent reviews, see Refs. [13, 14]). Now it is widely accepted that the driving force behind the MIT is the strong correlations between carriers. Here we study the metal–insulator transition and non-monotonic temperature-dependent resistivity on the metallic side near the MIT in the strongly-interacting two-valley 2D electron system in ultra-high mobility SiGe/Si/SiGe quantum wells in zero and spin-polarizing magnetic fields.

Measurements reported here were performed on ultra-high mobility SiGe/Si/SiGe quantum wells similar to those described in Refs. [15, 16]. The peak electron mobility, μ, in these samples reaches 240 $\mathrm{m}^2/\mathrm{V}\cdot\mathrm{s}$. It is important to note that judging by the appreciably higher quantum electron mobility ($\sim 10\ \mathrm{m}^2/\mathrm{V}\cdot\mathrm{s}$) in the SiGe/Si/SiGe quantum wells compared to that in Si MOSFETs, the residual disorder related to both short- and long-range random potential is drastically smaller

* E-mail: shashkin@issp.ac.ru
** E-mail: s.kravchenko@northeastern.edu

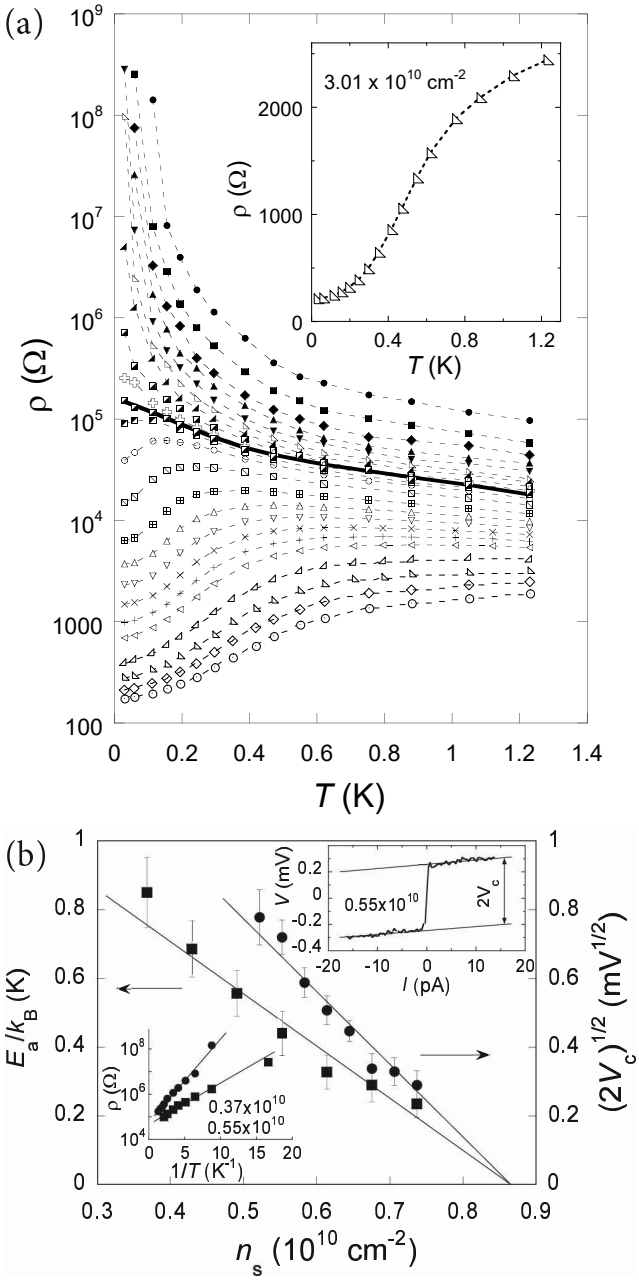

Fig. 1. (*a*) Temperature dependences of the resistivity in a SiGe/Si/SiGe quantum well in zero magnetic field. The electron densities in units of 10^{10} cm^{-2} (top to bottom) are: 0.37, 0.43, 0.49, 0.55, 0.61, 0.68, 0.74, 0.80, 0.85, 0.88, 0.92, 0.98, 1.17, 1.35, 1.54, 1.72, 1.90, 2.09, 2.27, 2.64, 3.01, 3.38, and 3.75. The solid line corresponds to the separatrix. The inset shows a close-up view of $\rho(T)$ at $n_s = 3.01{\cdot}10^{10}$ cm^{-2} displaying a drop of the resistivity by a factor of 12. (*b*) Activation energy and the square root of the threshold voltage as a function of the electron density in zero magnetic field. Vertical error bars correspond to the experimental uncertainty. The solid lines are linear fits yielding $n_c(0) = 0.87 \pm 0.02 \cdot 10^{10}$ cm^{-2}. Top inset: Current–voltage characteristic measured at a temperature of 30 mK. Bottom inset: Arrhenius plots of the resistivity in the insulating phase for two electron densities. The densities in both insets are indicated in cm^{-2}

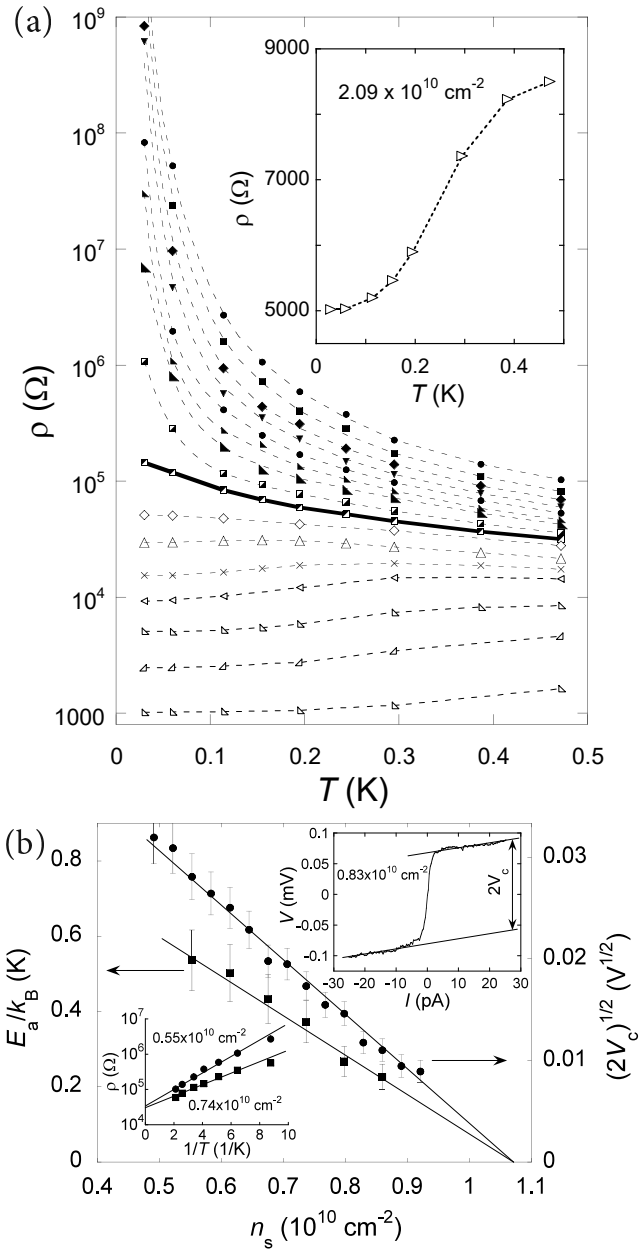

Fig. 2. (*a*) Resistivity of an electron system in a SiGe/Si/SiGe quantum well placed in the spin-polarizing magnetic field B^* as a function of temperature for electron densities (from top to bottom) 0.55, 0.61, 0.68, 0.74, 0.80, 0.86, 0.92, 1.01, 1.11, 1.22, 1.35, 1.54, 1.72, 2.09, 2.64, and $3.75 \cdot 10^{10}$ cm^{-2}. The solid line corresponds to the separatrix. The magnetic fields used are spanned in the range between approximately 1 and 2 T. The inset shows a closeup view of $\rho(T)$ for $n_s = 2.09 \cdot 10^{10}$ cm^{-2}. (*b*) Activation energy, E_a, and square root of the threshold voltage, $V_c^{1/2}$, vs electron density. Solid lines correspond to the best linear fits. Upper inset: a typical I–V dependence on the insulating side of the MIT at $T = 30$ mK. Lower inset: Arrhenius plots of the temperature dependence of the resistivity for two electron densities on the insulating side

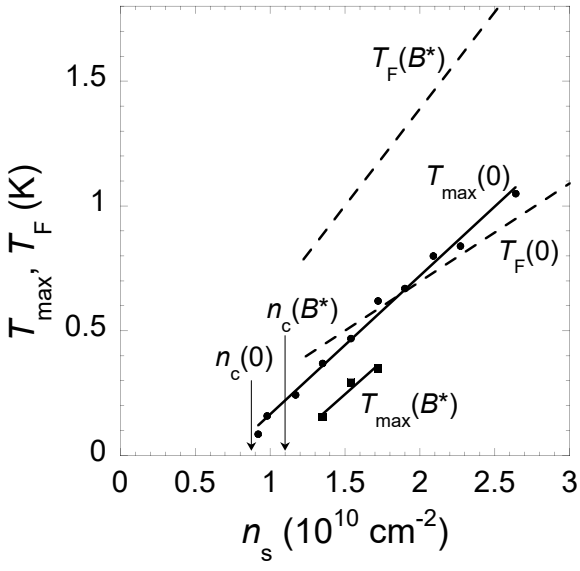

Fig. 3. T_{max} as a function of electron density in $B = 0$ (circles) and in $B = B^*$ (squares). Solid lines are linear fits. Critical electron densities for the metal–insulator transition in $B = 0$ and $B = B^*$ are indicated. Dashed lines show the Fermi temperatures T_F in $B = 0$ and $B = B^*$ calculated using the low-temperature value B^* and Eq. (1) from the full version of the paper

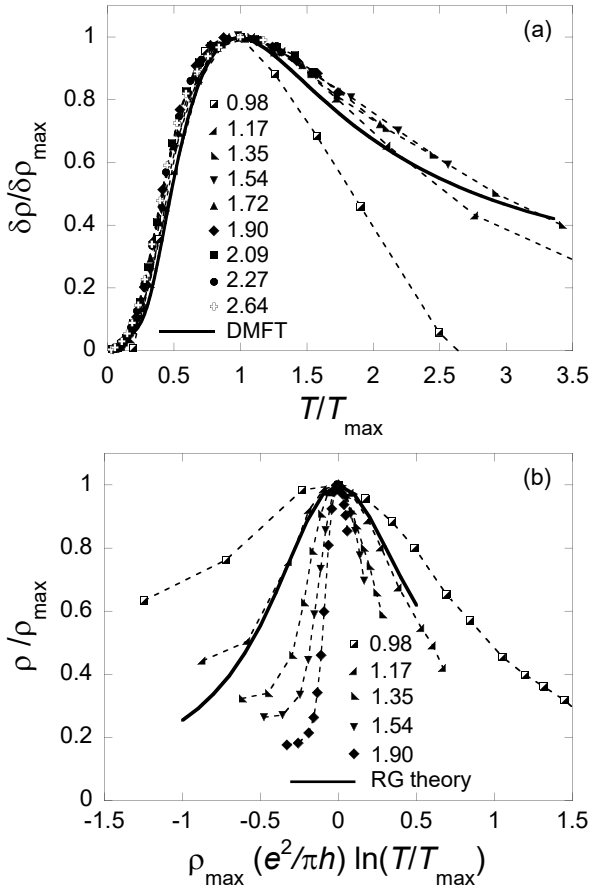

Fig. 4. (*a*) The ratio $(\rho(T) - \rho(0))/(\rho_{max} - \rho(0))$ as a function of T/T_{max} in $B = 0$. The solid line shows the result of the dynamical mean-field theory (DMFT) in the weak-disorder limit [37–39]. The electron densities are indicated in units of 10^{10} cm^{-2}. (*b*) The ratio ρ/ρ_{max} as a function of the product $\rho_{max} \ln(T/T_{max})$. The solid line is the result of the renormalization-group scaling theory [6, 7]

in the samples used here. The approximately 15 nm wide silicon (001) quantum well is sandwiched between $Si_{0.8}Ge_{0.2}$ potential barriers. The samples were patterned in Hall-bar shapes with the distance between the potential probes of 150 μm and width of 50 μm using standard photo-lithography. Measurements were carried out in an Oxford TLM-400 dilution refrigerator. Data on the metallic side of the transition were taken by a standard four-terminal lock-in technique in a frequency range 1–10 Hz in the linear response regime. On the insulating side of the transition, the resistance was measured with *dc* using a high input impedance electrometer. Since in this regime, the current–voltage (I–V) curves are strongly nonlinear, the resistivity was determined from dV/dI in the linear interval of I–V curves, as $I \to 0$.

The main part of the full version of the paper is organized as follows. In Sec. 2, using several independent methods, we find that the metal–insulator transition occurs in the strongly-interacting two-valley two-dimensional electron system in ultra-high mobility SiGe/Si/SiGe quantum wells in zero magnetic field. The MIT point and the resistivity drop with decreasing temperature are discussed comparatively to other electron systems. In Sec. 3, we show that the metallic state in ultra-low-disorder SiGe/Si/SiGe quantum wells survives in parallel magnetic fields strong enough to completely polarize the electrons' spins, thus making the electron system spinless. The behavior of the spinless electrons is discussed and compared to other electron systems. In Sec. 4, we find that the resistivity maximum temperature on the metallic side near the MIT in zero magnetic field in ultra-clean SiGe/Si/SiGe quantum wells is close to the renormalized Fermi temperature but decreases appreciably for spinless electrons in spin-polarizing magnetic fields, rather than increasing along with the Fermi temperature. The discrepancy with existing theories and the origin of the effect are discussed. In Sec. 5, we show that the low-temperature resistivity drop in both spin-unpolarized and spinless electron systems in ultra-clean SiGe/Si/SiGe quan-

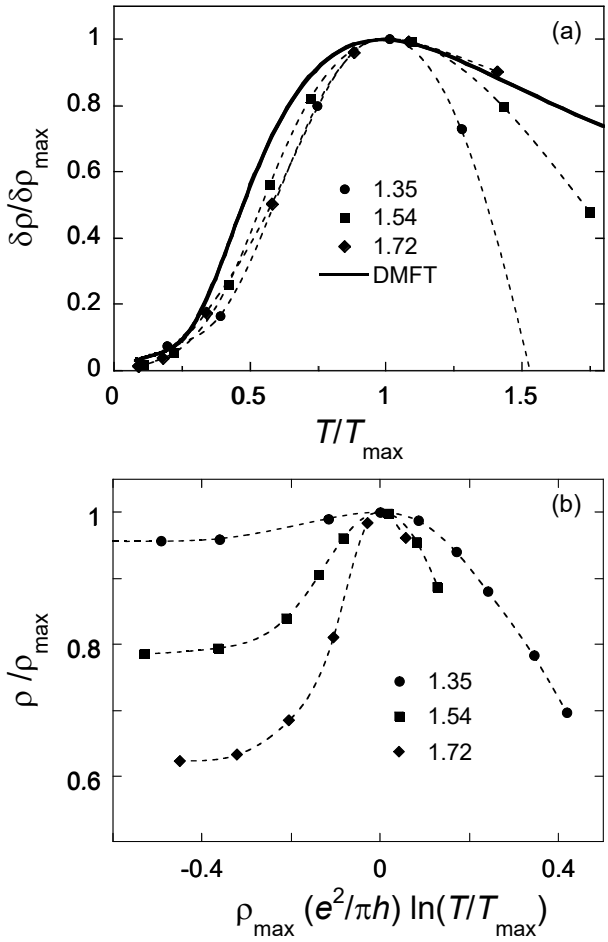

Fig. 5. (*a*) The ratio $\delta\rho/\delta\rho_{max}$ plotted as a function of T/T_{max} in $B = B^*$. The solid line is the result of DMFT in the weak-disorder limit [37–39]. The electron densities are indicated in units of 10^{10} cm^{-2}. (*b*) The analysis based on the scaling form suggested by the renormalization-group scaling theory [6, 7]

tum wells is described quantitatively by the dynamical mean-field theory.

The results are represented in Figs. 1–5.

The results and discussions are supported by Refs. [1–54].

6. Conclusions. We have found that the metal–insulator transition occurs in the strongly-interacting two-valley two-dimensional electron system in ultra-high mobility SiGe/Si/SiGe quantum wells in zero magnetic field and survives in the spinless system in spin-polarizing magnetic fields. In both cases, this is accompanied by the non-monotonic temperature-dependent resistivity on the metallic side near the transition. In zero magnetic field, the resistivity maximum temperature is found to be close to the renormalized Fermi temperature. However, rather than increasing along with the Fermi temperature, the value T_{max} decreases appreciably for spinless electrons in spin-polarizing magnetic fields. The observed behavior of T_{max} cannot be described by existing theories. The results indicate the spin-related origin of the effect. At the same time, the low-temperature resistivity drop in both spin-unpolarized and spinless electron systems is described quantitatively by the dynamical mean-field theory.

Funding. A. A. S. was supported by RSF Grant No. 22-22-00333. S. V. K. was supported by NSF Grant No. 1904024.

The full text of this paper is published in the English version of JETP.

REFERENCES

1. K. Behnia, Nat. Nanotechnol. **7**, 488 (2012).

2. Z. Zhu, A. Collaudin, B. Fauqué, W. Kang, and K. Behnia, Nat. Phys. **8**, 89 (2012).

3. J. R. Schaibley, H. Yu, G. Clark, P. Rivera, J. S. Ross, K. L. Seyler, W. Yao, and X. Xu, Nat. Rev. Mater. **1**, 16055 (2016).

4. Z. Zhu, J. Wang, H. Zuo, B. Fauqué, R. D. McDonald, Y. Fuseya, and K. Behnia, Nat. Commun. **8**, 15297 (2017).

5. P. A. Lee and T. V. Ramakrishnan, Rev. Mod. Phys. **57**, 287 (1985).

6. A. Punnoose and A. M. Finkel'stein, Phys. Rev. Lett. **88**, 016802 (2001).

7. A. Punnoose and A. M. Finkel'stein, Science **310**, 289 (2005).

8. G. Fleury and X. Waintal, Phys. Rev. Lett. **101**, 226803 (2008).

9. T. N. Zavaritskaya and É. I. Zavaritskaya, JETP Lett. **45**, 609 (1987).

10. S. V. Kravchenko, G. V. Kravchenko, J. E. Furneaux, V. M. Pudalov, and M. D'Iorio, Phys. Rev. B **50**, 8039 (1994).

11. S. V. Kravchenko, W. E. Mason, G. E. Bowker, J. E. Furneaux, V. M. Pudalov, and M. D'Iorio, Phys. Rev. B **51**, 7038 (1995).

12. D. Popović, A. B. Fowler, and S. Washburn, Phys. Rev. Lett. **79**, 1543 (1997).

13. A. A. Shashkin and S. V. Kravchenko, Appl. Sci. **9**, 1169 (2019).

14. A. A. Shashkin and S. V. Kravchenko, Ann. Phys. **435**, 168542 (2021).

15. M. Y. Melnikov, A. A. Shashkin, V. T. Dolgopolov, S.-H. Huang, C. W. Liu, and S. V. Kravchenko, Appl. Phys. Lett. **106**, 092102 (2015).

16. M. Y. Melnikov, V. T. Dolgopolov, A. A. Shashkin, S.-H. Huang, C. W. Liu, and S. V. Kravchenko, J. Appl. Phys. **122**, 224301 (2017).

17. Y. Hanein, U. Meirav, D. Shahar, C. C. Li, D. C. Tsui, and H. Shtrikman, Phys. Rev. Lett. **80**, 1288 (1998).

18. P. Brussarski, S. Li, S. V. Kravchenko, A. A. Shashkin, and M. P. Sarachik, Nat. Commun. **9**, 3803 (2018).

19. A. A. Shashkin, S. V. Kravchenko, V. T. Dolgopolov, and T. M. Klapwijk, Phys. Rev. B **66**, 073303 (2002).

20. A. Mokashi, S. Li, B. Wen, S. V. Kravchenko, A. A. Shashkin, V. T. Dolgopolov, and M. P. Sarachik, Phys. Rev. Lett. **109**, 096405 (2012).

21. M. Y. Melnikov, A. A. Shashkin, V. T. Dolgopolov, A. Y. X. Zhu, S. V. Kravchenko, S.-H. Huang, and C. W. Liu, Phys. Rev. B **99**, 081106(R) (2019).

22. D. G. Polyakov and B. I. Shklovskii, Phys. Rev. B **48**, 11167 (1993).

23. A. A. Shashkin, V. T. Dolgopolov, and G. V. Kravchenko, Phys. Rev. B **49**, 14486 (1994).

24. A. A. Shashkin, S. V. Kravchenko, and T. M. Klapwijk, Phys. Rev. Lett. **87**, 266402 (2001).

25. T. Ando, A. B. Fowler, and F. Stern, Rev. Mod. Phys. **54**, 437 (1982).

26. A. A. Shashkin, A. A. Kapustin, E. V. Deviatov, V. T. Dolgopolov, and Z. D. Kvon, Phys. Rev. B **76**, 241302 (2007).

27. M. Y. Melnikov, A. A. Shashkin, V. T. Dolgopolov, S.-H. Huang, C. W. Liu, A. Y. X. Zhu, and S. V. Kravchenko, Phys. Rev. B **101**, 045302 (2020).

28. T. Okamoto, K. Hosoya, S. Kawaji, and A. Yagi, Phys. Rev. Lett. **82**, 3875 (1999).

29. S. A. Vitkalov, H. Zheng, K. M. Mertes, M. P. Sarachik, and T. M. Klapwijk, Phys. Rev. Lett. **85**, 2164 (2000).

30. X. P. A. Gao, G. S. Boebinger, A. P. Mills, Jr., A. P. Ramirez, L. N. Pfeiffer, and K. W. West, Phys. Rev. B **73**, 241315(R) (2006).

31. V. T. Dolgopolov, A. A. Shashkin, and S. V. Kravchenko, Phys. Rev. B **96**, 075307 (2017).

32. A. M. Finkel'stein, Sov. Phys. JETP **57**, 97 (1983).

33. A. M. Finkel'stein, Z. Phys. B **56**, 189 (1984).

34. C. Castellani, C. Di Castro, P. A. Lee, and M. Ma, Phys. Rev. B **30**, 527 (1984).

35. A. Punnoose, A. M. Finkel'stein, A. Mokashi, and S. V. Kravchenko, Phys. Rev. B **82**, 201308(R) (2010).

36. S. Anissimova, S. V. Kravchenko, A. Punnoose, A. M. Finkel'stein, and T. M. Klapwijk, Nat. Phys. **3**, 707 (2007).

37. A. Camjayi, K. Haule, V. Dobrosavljević, and G. Kotliar, Nat. Phys. **4**, 932 (2008).

38. M. M. Radonjić, D. Tanasković, V. Dobrosavljević, K. Haule, and G. Kotliar, Phys. Rev. B **85**, 085133 (2012).

39. V. Dobrosavljević and D. Tanasković, in *Strongly Correlated Electrons in Two Dimensions*, ed. by S. V. Kravchenko, Pan Stanford Publ. (2017), ch. 1, p. 1–46.

40. A. A. Shashkin, M. Y. Melnikov, V. T. Dolgopolov, M. M. Radonjić, V. Dobrosavljević, S.-H. Huang, C. W. Liu, A. Y. X. Zhu, and S. V. Kravchenko, Phys. Rev. B **102**, 081119(R) (2020).

41. B. Spivak, Phys. Rev. B **67**, 125205 (2003).

42. B. Spivak and S. A. Kivelson, Phys. Rev. B **70**, 155114 (2004).

43. B. Spivak and S. A. Kivelson, Ann. Phys. **321**, 2071 (2006).

44. A. A. Shashkin, M. Y. Melnikov, V. T. Dolgopolov, M. M. Radonjić, V. Dobrosavljević, S.-H. Huang, C. W. Liu, A. Y. X. Zhu, and S. V. Kravchenko, Sci. Rep. **12**, 5080 (2022).

45. M. Y. Melnikov, A. A. Shashkin, V. T. Dolgopolov, S.-H. Huang, C. W. Liu, and S. V. Kravchenko, Sci. Rep. **7**, 14539 (2017).

46. A. A. Shashkin, S. Anissimova, M. R. Sakr, S. V. Kravchenko, V. T. Dolgopolov, and T. M. Klapwijk, Phys. Rev. Lett. **96**, 036403 (2006).

47. O. Prus, Y. Yaish, M. Reznikov, U. Sivan, and V. Pudalov, Phys. Rev. B **67**, 205407 (2003).

48. V. T. Dolgopolov and A. Gold, Phys. Rev. Lett. **89**, 129701 (2002).

49. A. Gold and V. T. Dolgopolov, J. Phys. Condens. Matter **14**, 7091 (2002).

50. A. A. Shashkin, Phys. Usp. **48**, 129 (2005).

51. N. Teneh, A. Y. Kuntsevich, V. M. Pudalov, and M. Reznikov, Phys. Rev. Lett. **109**, 226403 (2012).

52. V. M. Pudalov, A. Y. Kuntsevich, M. E. Gershenson, I. S. Burmistrov, and M. Reznikov, Phys. Rev. B **98**, 155109 (2018).

53. S. V. Kravchenko and M. P. Sarachik, Rep. Prog. Phys. **67**, 1 (2004).

54. T. M. Lu, W. Pan, D. C. Tsui, P. C. Liu, Z. Zhang, and Y. H. Xie, Phys. Rev. Lett. **107**, 126403 (2011).